Journal of Urban and Environmental Engineering, v.5, n.2, p.91-102

ISSN 1982-3932
doi: 10.4090/juee.2011.v5n2.091102

Journal of Urban and Environmental Engineering

www.journal-uee.org

INFLUENCE OF THE CATCHMENT DISCRETIZATION ON THE OPTIMIZATION OF RUNOFF-EROSION MODELLING

Celso A.G. Santos[1*], Paula K.M.M. Freire[1], Richarde M. da Silva[2], Petley M. Arruda[1] and Sudhanshu K. Mishra[3]

[1] *Department of Civil and Environmental Engineering, Federal University of Paraíba, 58051-900 João Pessoa, Paraíba, Brazil*

[2] *Department of Geosciences, Federal University of Paraíba, 58051-900 João Pessoa, Paraíba, Brazil*

[3] *Department of Economics, North-Eastern Hill University, Shillong, India*

Received 7 November 2011; received in revised form 6 December 2011; accepted 28 December 2011

Abstract: In this application-based study, the influence of the catchment discretization on the optimization of runoff-erosion modeling using a particle swarm optimization to a physically-based erosion model named WESP (Watershed Erosion Simulation Program) is conducted. This study is carried in the semiarid region of Brazil, more precisely in a micro-catchment (MCN3) of Sumé Experimental Basin. A comparative assessment is done by statistical analysis and mean relative error (MRE) in order to evaluate the performance of the optimization technique when discretizing the catchment in different ways. Thus, the catchment is represented in three ways of discretization (i.e., n_1 = 4 elements, n_2 = 10 elements and n_3 = 23 elements). The difficulties involved in calibration of physically-based erosion models have been partly attributable to the lack of robust optimization tools, hence several robust optimization techniques have been proposed in the past years; however, the way the catchment is represented could interfere on the results. Thus, this paper presents the essential concepts of the runoff-erosion WESP model, the global optimization method known as Repulsive Particle Swarm (RPS), and the optimization results using the three catchment discretization. The results show that there are small differences among the calculated sediment yield using the three ways of basin discretization, although the 23 elements division seems to give the best results.

Keywords: Discretization; optimization; runoff-erosion modeling; semiarid area

[*] Correspondence to: Celso A. G. Santos. E-mail: celso@ct.ufpb.br

INTRODUCTION

The degradation of water quality and quantity are among the major environmental problems, which the society is facing today. Environmental managers use computer modeling to simulate and to better understand the natural phenomena that occur in watersheds, in order to assist the planning of the use and preservation of natural resources.

In recent years, computer-based runoff-erosion models have become a useful tool for water-resources management, flood forecasting and control, and environmental concerns. For those applications, a certain level of accuracy and reliability is expected from these models in their ability to describe the hydrologic response of a catchment. The influence and importance of spatial scale on rainfall-runoff modeling has long been recognized. With the advances in computer capability and availability, an increasing number of hydrologic engineers have changed from using basin-based, lumped-system hydrologic models to physically-based, distributed-system models (Mazion Jr. & Yen, 1994). This change in modeling approach reflects a general desire to increase the accuracy and capability to describe the hydrologic responses of a catchment.

The parameterization of runoff-erosion models is an important but difficult task because many of the parameters in these models are not directly measurable in the field and therefore can only be obtained through calibration against a historical record of data. Model calibration consists of tuning the values of unknown or partially known model parameters, such that the model predictions fit as closely and consistently as possible to the observations. This can be done by visual adjustment but the subjective and time-consuming nature of the trial-and-error method makes this approach difficult for models with a large number of parameters. In this widely encountered case, an automatic calibration procedure is necessary (Laloy *et al.*, 2010; Soares Júnior *et al.*, 2010b; Santos *et al.*, 2011a; Santos *et al.*, 2011b).

Estimating direct runoff-erosion from a catchment is important both from water quantity and quality standpoints. In this regard, the use of erosion models has gained wider acceptance over lumped models because of their ability to handle spatial variability of both climatic and topographic parameters. However, distributed models tend to be more complex and typically need a large number of parameters that need to be estimated or measured (Kalin *et al.*, 2003). As the spatial scale of the catchment increases, modeling hydrologic processes of runoff-erosion and surface erosion become more complex.

Currently, catchment delineation and stream network extraction are accomplished by utilizing Geographic Information Systems and Digital Elevation Models. The most common method of extracting channel networks is by specifying a Critical Source Area (CSA) required for initiating a channel. However, the results after extraction are very sensitive to this threshold value (Morris & Heerdegen, 1988; Kalin *et al.*, 2003). The specification of the CSA has been based on geomorphologic laws (Tarboton *et al.*, 1991), scaling invariance of probability distributions of channel network attributes (Tarboton *et al.*, 1988; Rodriguez-Iturbe *et al.*, 1992; Rigon *et al.*, 1993), local slope (Kalin *et al.*, 2003) and critical shear stress (Rinaldo *et al.*, 1995) and terrain curvature.

Some studies have used both geomorphologic properties and hydrologic responses for determining CSAs (Helmlinger *et al.*, 1993; Gandolfi & Bischetti, 1997). However, the assumptions of constant threshold areas and how they are influenced by morphometric and scaling properties are often not met in natural watersheds (Snell & Sivapalan, 1994).

Another approach to identify the appropriate CSA for channel extraction are exposed in Thieken *et al.* (1999), which utilized the Kineros model to evaluate data aggregation on catchment response from synthetic rainfall events. Zhang & Montgomery (1994) suggested a spatial resolution of 10 m to represent hydrologic processes based on simulations with Topmodel. Vieux & Needham (1993) investigated the sensitivity of a nonpoint-pollution model (AGNPS) to grid cell size. Bingner *et al.* (1997) evaluated the effect of various levels of catchment subdivision and sub-catchment size on simulated annual sediment yield of fine material based on simulations with the SWAT model.

All of the above studies analyzed the impact of watershed subdivision or the selection of the threshold area on runoff hydrograph alone, and did not consider sediment yield. These studies reported a minimal improvement in prediction of sediment yield beyond a certain number sub-catchment.

The major problem concerning the use of physically-based model in erosion prediction is the need of parameters which cannot be directly measured in the field. In this context, many algorithms for function optimization are employed to find values for those parameters. However, it is difficult to assure that the final value for the parameter is not a result of either a local minimum or another trap. Therefore, more robust algorithms are required to estimate the parameter's final value (Soares Júnior *et al.*, 2010a; Santos *et al.*, 2011b).

Repulsive Particle Swarm (RPS) is a population based stochastic optimization technique, inspired by social behavior of bird flocking or fish schooling. It shares many similarities with evolutionary computation techniques such as Genetic Algorithms (Santos *et al.*, 2003). The system is initialized with a population of random solutions and searches for optima by updating generations.

Recently, such a type of optimization technique has shown promise as an effective and efficient optimization algorithm for calibrating catchment

models. This paper presents the essential concepts of the RPS and of the physically-based runoff-erosion WESP model, with the main objective of verifying the influence of the catchment discretization on the optimization of WESP model.

WESP MODEL

Lopes & Lane (1988) developed a physically-based distributed model called Watershed Erosion Simulation Program (WESP), which computes runoff and sediment yield based on kinematic waves approximation for the surface flow due to excess rainfall r_e (m/s), which is obtained by the subtraction of the infiltration rate $f(t)$ from the rainfall intensity I, i.e., $r_e = I - f(t)$. The model was developed for small basins to generate the hydrograph and the respective sedigraph. The infiltration process is modeled with the Green-Ampt equation (Green & Ampt, 1911), which can be written in the form:

$$f(t) = K_s\left(1+\frac{\Delta\theta\psi}{F(t)}\right) \quad (1)$$

where, K_s is the effective saturated soil hydraulic conductivity (m/s), $F(t)$ is the cumulative depth of infiltrated water (m), ψ is the average suction head at the wetting front (m), $\Delta\theta$ is the change in the moisture content, and t is the time variable (s). The moisture content θ and suction head ψ may be expressed as a single parameter that can be called moisture-tension parameter N_s, such that:

$$N_s = \Delta\theta\psi_i = (\theta_s - \theta_i)\psi_i \quad (2)$$

where θ_s is the soil moisture content at saturation, which is almost equal to the soil porosity and θ_i is the initial soil moisture content. The surface flow is considered to be either the overland flow on planes or channel flow.

Overland flow

The spatially varied overland flow is considered one-dimensional and is described by Manning's turbulent flow equation:

$$u = \frac{1}{n}R_H^{2/3}S_f^{1/2} \quad (3)$$

where u is the local mean flow velocity (m/s), $R_H(x,t)$ is the hydraulic radius (m), S_f is the friction slope and n is the Manning friction factor. Thus, the local velocity for plane flow can be obtained considering the hydraulic radius equal to the depth of flow ($R_H = h$) and using the kinematic wave approximation resulting in the friction slope being equal to the plane slope ($S_0 = S_f$) as:

$$u = \alpha h^{m-1} \quad (4)$$

where h is the depth of flow (m), α is a parameter related to surface slope and roughness, equal to $(1/n)S_0^{1/2}$, and m is a geometry parameter whose value is set to 5/3 for wide rectangles.

The equation of continuity for the one-dimensional plane can, then, be written as:

$$\frac{\partial h}{\partial t} + \alpha m h^{m-1}\frac{\partial h}{\partial x} = r_e \quad (5)$$

From **Eqs 4–5**, the overland flow velocity and depth (u, h) can be calculated for a given rainfall excess r_e. The beginning of surface runoff is obtained by determining the pounding time (t_p) for an unsteady rain.

Sediment transport is considered as the erosion rate in the plane reduced by the deposition rate within the reach. The erosion occurs due to raindrop impact as well as surface shear. Thus, the continuity equation for sediment transport is expressed as:

$$\frac{\partial(ch)}{\partial t} + \frac{\partial(cuh)}{\partial x} = e_I + e_R - d \quad (6)$$

where c is the sediment concentration in the surface flow (kg/m³), e_I is the rate of sediment erosion due to rainfall impact (kg/m²/s), e_R is the erosion rate due to shear stress (kg/m²/s), and d is the rate of sediment deposition (kg/m²/s).

The rate of sediment erosion due to rainfall impact e_I is a function of the rate of detachment by raindrop impact and the rate of transport of sediment particles by shallow flow. A simple functional form of detachment by raindrop impact could use rainfall intensity as a measure of the erosivity of raindrop impact (Foster, 1982), and in order to include the process of sediment transport by shallow flow on hillslopes, Lane and Shirley (1985) included rainfall and expressed e_I as:

$$e_i = K_I I r_e \quad (7)$$

where K_I is the soil detachability parameter (kg·s/m⁴). The rate of sediment erosion due to shear stress e_R is expressed by an entrainment rate proportional to a power of the average shear stress acting on the soil surface (Croley II, 1982; Foster, 1982) as:

$$e_r = K_r \tau^{1.5} \quad (8)$$

where K_r is a soil erodibility factor for shear (kg·m/N$^{1.5}$·s), and τ is the effective shear stress (N/m²), which is given by $\tau = \gamma h S_f$, γ being the specific weight

of water (N/m^3). Entrainment and transport of sediment occur when the erosive forces exceed the resisting forces.

Water flowing over the soil surface exerts shear forces on the soil particles that tend to move or entrain them. On bare soil surface and stream beds, the forces that resist the erosion by flowing water depend on the size and the distribution of the sediment particles. For coarse sediments, the forces resisting entrainment are mainly frictional forces that depend on the weight of the particles.

Finer sediments that contain appreciable fractions of silt or clay, or both, tend to be cohesive and resist entrainment due mainly to cohesion than friction. Also, in fine sediments groups of particles (aggregates) get entrained as single units whereas coarse noncohesive sediments are moved as individual particles. Thus, the amount of entrainment is related to the magnitude of total shear stress as expressed in **Eq. (8)** rather than to a "critical" shear stress. Finally, the rate of sediment deposition d in **Eq. (6)** is not only the deposition of the particular sediment per unit of area and per unit of time, but it also represents the rate at which the column of suspension loses solids per unit of time, and is expressed as (Einstein, 1968):

$$d = \varepsilon_p V_s c \tag{9}$$

where ε_p is a coefficient that depends on the sediment and fluid properties, set to 0.5 in the present study based on Davis (1978), $c(x,t)$ is the plane sediment concentration in transport (kg/m^3), and V_s is the particle fall velocity (m/s) computed by Rubey's equation:

$$V_s = F_o \sqrt{\frac{(\gamma_s - \gamma)}{\gamma} g d_s} \tag{10}$$

and,

$$F_o = \sqrt{\frac{2}{3} + \frac{36\nu^2}{g d_s^3 \left(\frac{\gamma_s}{\gamma} - 1\right)}} - \sqrt{\frac{36\nu^2}{g d_s^3 \left(\frac{\gamma_s}{\gamma} - 1\right)}} \tag{11}$$

where γ_s is the specific weight of sediment (N/m^3), ν is the kinematic viscosity of water (m^2/s), d_s is the mean diameter of the sediment (m), and g is the acceleration of gravity (m/s^2).

Channel flow

The concentrated flow in the channels is also described by continuity and momentum equations. The momentum equation can be reduced to the discharge equation with the kinematic wave approximation as:

$$Q = \alpha A R_H^{m-1} \tag{12}$$

where Q is the discharge (m^3/s), and A is the cross-sectional area of flow (m^2). The continuity equation for the channel flow is given by:

$$\frac{\partial A}{\partial t} + \frac{\partial Q}{\partial x} = q_A \tag{13}$$

where q_A is the lateral inflow per unit length of channel. **Equations 12–13** enable the calculation of channel flow.

Since the effect of rainfall impact is negligible in the channel, the continuity equation for the sediment is expressed without the rainfall impact component by:

$$\frac{\partial AC}{\partial t} + \frac{\partial CQ}{\partial x} = q_s + e_r - d_c \tag{14}$$

where $C(x,t)$ is the sediment concentration in transport in the channel (kg/m^2), q_s is the lateral sediment inflow into the channel (kg/m/s), d_c is the rate of sediment deposition in the channel (kg/m/s), and e_r is the erosion rate of the channel bed material (kg/m/s). The components of the net sediment flux for the channel segment are given as follows: the erosion rate of the channel bed material e_r is obtained from a general equation, initially developed for bed-load transport capacity (Croley II, 1982; Foster, 1982):

$$e_r = a\left(\tau - \tau_c\right)^{1.5} \tag{15}$$

where a is the sediment erodibility parameter, and τ_c is the critical shear stress for sediment entrainment (N/m^2), which is given by $\tau_c = \delta(\gamma_s - \gamma)d_s$, where δ is a coefficient, set to 0.047 in the present study, γ_s is the specific weight of sediment (N/m^3), and d_s is the mean diameter of sediments (m).

The rate of sediment deposition within the channel d_c (kg/m/s) in equation (14) is expressed by (Mehta, 1983):

$$d_c = \varepsilon_c T_W V_s C \tag{16}$$

where ε_c is the deposition parameter for channels, considered as unity in the present case based on the study of Einstein (1968), and T_W is the top width of the channel flow (m).

From equation (14), sediment transport rate (CQ) can be calculated for the overland flow with A and Q obtained from **Eq. (13)**.

REPULSIVE PARTICLE SWARM

The Repulsive Particle Swarm (RPS) proposed by Urfalioglu (2004) is a method of optimization that is a variant of the particle swarm optimization (PSO)

(Santos *et al.*, 2010). It is particularly effective in finding out the global optimum in very complex search spaces; although, it may be slower on certain types of optimization problems.

The particle swarm optimization (PSO) was invented by Eberhart & Kennedy (1995) inspired by simulating the behavior of birds. This method is an instance of a successful application of the philosophy of bounded rationality and decentralized decision-making to solve the global optimization problems (Simon, 1982). It is observed that a swarm of birds or insects or a school of fish searches for food, protection, etc. in a very typical manner. If one of the members of the swarm sees a desirable path to go, the rest of the swarm will follow quickly.

Every member of the swarm searches for the best in its locality and learns from its own experience. Additionally, each member learns from the others, especially from the best performer among them. Even human beings show a tendency to learn from their own experience, their immediate neighbors and the ideal performers. The particle swarm method of optimization mimics the said behavior. Every individual of the swarm is considered as a particle in a multidimensional space that has a position and a velocity. The particles fly through hyperspace and remember the best position that they have seen. Members of a swarm communicate the good positions to each other and adjust their own position and velocity based on these good positions. There are two main ways this communication is done: (i) "swarm best" that is known to all, (ii) "local bests" are known in neighbourhoods of particles. Updating the position and velocity is done at each iteration as follows:

$$v_{i+1} = \omega v_i + c_1 r_1(\hat{x}_i - x_i) + c_2 r_2(\hat{x}_{gi} - x_i) \qquad (17)$$

$$x_{i+1} = x_i + v_{i+1} \qquad (18)$$

where x is the position and v is the velocity of the individual particle, the subscripts i and $i + 1$ stand for the recent and the next (future) iterations, respectively; w is the inertial constant, good values are usually slightly less than 1; c_1 and c_2 are constants that say how much the particle is directed towards good positions, Good values are usually right around 1. Further, r_1 and r_2 are random values in the range [0, 1], $\hat{x}_i$ is the best that the particle has attained in the past, $\hat{x}_g$ is the global best seen by the swarm. This can be replaced by $\hat{x}_L$, the local best, if neighborhoods are being used.

The traditional RPS gives little scope of local search to the particles. They are guided by their past experience and the communication received from the others in the swarm. We have modified the traditional RPS method by endowing stronger (wider) local search ability to each particle. Each particle flies in its local surrounding and searches for a better solution. The domain of its search is controlled by a new parameter (*nstep*). This local search has no preference to gradients in any direction and closely resembles tunnelling. This added exploration capability of the particles brings the RPS method closer to what is observed in real life. However, in some cases, a moderately wide search (e.g. *nstep* = 9) works better. It has been said that each particle learns from its "chosen" inmates in the swarm. Now, at the one extreme is to learn from the best performer in the entire swarm.

This is how the particles in the original PS method learn. However, such learning is not natural. It is neither expected nor even feasible that an individual knows of the best performer in the population and interacts with all others in the swarm, and therefore relies only on the possibility of a limited interaction and limited knowledge that any individual can possess and acquire. Then, our particles do not know the "best" in the swarm. Nevertheless, they interact with some chosen inmates that belong to the swarm. Now, the issue is: how does the particle choose its inmates? One of the possibilities is that it chooses the inmates nearer to it. But, since our particle explores the locality by itself, it is likely that it would not benefit much from the inmates closer to it. Other relevant topologies are (the celebrated) ring topology, ring topology hybridized with random topology, star topology, von Neumann topology, etc.

Let us visualize the possibilities of choosing (a predetermined number of) inmates randomly from among the members of the swarm. This is much closer to reality in the human world. When we are exposed to the mass media, we experience this. Alternatively, we may visualize our particles visiting a public place, (e.g. railway platform, church, etc.) where it (he) meets people coming from different places. Here, geographical distance of an individual from the others is not important. Important is how the experiences of others are communicated to us. There are large many sources of such information, each one being selective in what it broadcasts and each of us selective in what we attend to and, therefore, receive. This selectiveness at both ends transcends the geographical boundaries and each one of us is practically exposed to randomized information. Of course, two individuals may have a few common sources of information.

We have used these arguments in the scheme of dissemination of others' experiences to each individual particle. Presently, we have assumed that each particle chooses a pre-assigned number of inmates (randomly) from among the members of the swarm. However, this number may be randomized to lie between two pre-assigned limits.

Calibration and simulations

In the WESP model, the catchment is represented as a cascade of planes and channels. Among the various

parameters involved in the plane and channel processes, the values of some are known, some are adopted *a priori*, and the rest are determined by calibration. Santos et al. (2005) used a representation of 10 elements made up of seven planes and three channels for the selected micro-catchment in the Sumé Experimental Basin.

The parameters which are fixed *a priori* are the Manning friction factor, which was assumed as 0.02 for planes and 0.03 for channels based on the soil type, its grain size composition and surface characteristics, the specific weight of water (9.8 kN/m³), and the specific weight of sediment (2.6×10^4 N/m³). However, there are some parameters that are specific for this area which should be determined by field tests such as the saturated soil hydraulic conductivity K_s whose average value was set equal to 5.0 mm/h and the mean diameter of sediments d_s whose value was assumed to be equal to d_{50} (0.5 mm). The other parameter values should be based either on the literature or determined by calibration with an optimization process.

The moisture-tension parameter N_s in **Eq. 2** was calibrated by a simple trial-and-error method, since it is the only parameter which controls the runoff process. However, there are three parameters in the WESP model to be determined by optimization (a, K_r and K_l). Theses parameters are related to the erosion process, so the optimization had to be done according to the adjustment of calculated and observed sediment yield data. Since there are no universally applicable values for these three erosion parameters, they were optimized using the RPS method using the following objective function:

$$J = \frac{|E_o - E_c|}{E_o} \qquad (19)$$

where J is objective function, E_o is observed sediment yield (kg/ha) and E_c is calculated sediment yield (kg/ha).

Study area and micro-catchment discretization

The studied micro-catchment (MCN3) is located in the sub-catchment Umburana (10.7 km² area) and inserted in Sumé Experimental Basin, 137.4 km² area (**Fig. 1**). The climate of the region is typically semiarid with irregular rainfall and a mean annual precipitation of 590 mm. The soil cover is relatively thin underlain by the bed rock. The predominant soil is brown non calcic-vertic occurring in more than 85% of the basin area (Srinivasan & Galvão, 1995).

The field installations consist of four micro-catchments varying in area from 0.48 to 1.07 ha, with all of them designed to permit the measurement of total surface runoff and erosion losses from the area. Two of the micro-catchments are maintained with natural undisturbed vegetation.

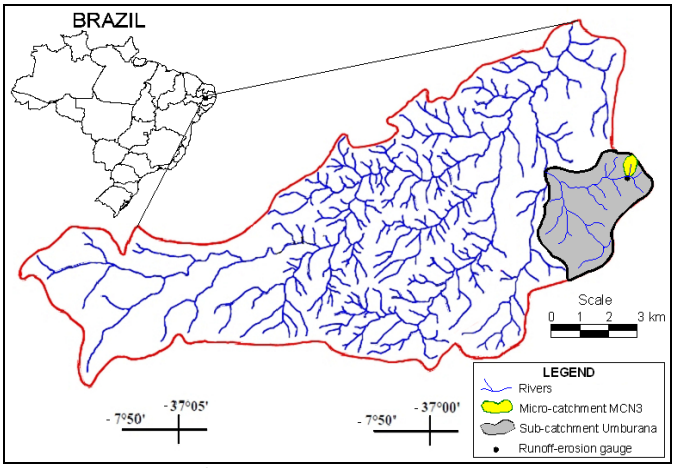

Fig. 1 Location of the micro-catchment MCN3 in Umburana catchment and Sumé Experimental Basin.

The other two were completely cleared and are maintained with bare soil surface. A detailed description of the procedure for obtaining data and the field measurements has been provided elsewhere (Cadier *et al.*, 1983; Srinivasan *et al.*, 1988).

In this study, it was used the micro-catchment number 3 (MCN3). The MCN3 has an area of 0.52 ha, perimeter of 302 m, mean slope 7.1%, and bare soil. In the case of micro-catchment, the runoff hydrograph and the total soil loss could be obtained. **Table 1** and **Figs 2–3** present the different divisions of the MCN3 in planes and channels elements. The MCN3 was represented in three ways of discretization with 4, 10 and 23 elements.

The relative efficiency of the model was assessed by the widely-used Nash-Sutcliffe R^2 efficiency index (Nash & Sutcliffe, 1970) and the mean relative error (Elshorbagy *et al.*, 2000). For the purpose of this study, the MRE is defined as the average of the absolute values of the errors between the estimated and the observed sediment yield expressed as fractions of the corresponding observed sediment yield. Although the WESP model in each test with each optimization method is calibrated for obtaining the best performance over the calibration period, the relative efficiencies of the optimization method is determined on the basis of their corresponding performances in verification and on the degree of variability of the parameter values in successive tests.

APPLICATION AND RESULTS

Setting of the RPS parameters

The RPS method of optimization contains some probabilistic and deterministic components which are controlled by some algorithmic parameters. For the method to perform optimally, these parameters must be chosen carefully. The following set of parameters was used in the present work: (N = 100, NN = 40, MX = 100, $NSTEP$ = 15, $ITRN$ = 1, $NSIGMA$ = 1, $ITOP$ = 3), in which N is the population size. In most of the

Table 1. Different discretizations of the MCN3 in plane and channel elements

Discretization n_1				
Element	Area (m²)	Length (m)	Width (m)	Slope
1	2 169	41.20	52.64	0.085
2	1 573	30.00	52.43	0.090
3	1 458	35.00	41.66	0.105
4	–	16.53	–	0.050
Discretization n_2				
Element	Area (m²)	Length (m)	Width (m)	Slope
1	2 166.66	41.18	52.60	0.0896
2	349.12	34.87	10.02	0.0936
3	434.45	34.67	12.52	0.0998
4	–	23.04	–	0.0554
5	931.36	41.33	22.54	0.0806
6	447.00	35.67	12.52	0.0903
7	–	23.04	–	0.0466
8	278.85	27.85	10.02	0.0791
9	592.56	39.43	15.03	0.0878
10	–	16.53	–	0.0665
Discretization n_3				
Element	Area (m²)	Length (m)	Width (m)	Slope
1	262.00	10.0	26.2	0.080
2	225.00	7.5	30.0	0.080
3	662.20	22.0	30.1	0.057
4	–	46.0	–	0.078
5	162.50	6.5	25.0	0.030
6	325.00	13.0	25.0	0.028
7	–	35.0	–	0.085
8	182.00	26.0	7.0	0.076
9	–	5.0	–	0.080
10	302.50	11.0	27.5	0.090
11	180.00	8.0	22.5	0.063
12	–	27.5	–	0.073
13	463.75	26.5	17.5	0.091
14	235.50	15.0	15.7	0.133
15	206.72	13.6	15.2	0.059
16	219.80	14.0	15.7	0.143
17	–	15.7	–	0.060
18	508.80	24.0	21.2	0.071
19	612.50	25.0	24.5	0.080
20	–	24.5	–	0.049
21	223.86	12.3	18.2	0.090
22	378.00	16.8	2.5	0.085
23	–	20.0	–	0.04

cases $N = 30$ works well but its value may be increased to 50 or 100.

The parameter *NN* is the size of randomly chosen neighbors, which ranges from 15 to 25 (but sufficiently less than N) is a good choice. The parameter *MX* is the maximal size of decision variables. In $f(x_1, x_2,..., x_m)$, m' should be less than or equal to *MX*. The parameter *ITRN* is the number of iterations. It may depend on the problem. Commonly, the range from 200 (at least) to 500 iterations may be good enough. But for functions like Rosenbrock or Griewank of large size (say $m' = 30$) it is needed that *ITRN* is large, say 5000 or even 10 000. Exceptionally, the *ITRN* was set to 1 in order to gain in time execution and the results were satisfactory enough. *ITOP* less than or equal to 1 means a ring topology, *ITOP* equal to 2 means a ring and random topology, and *ITOP* larger than or equal to 3 means a random topology. If *NSIGMA* is equal to 0, it means no chaotic perturbation, and when it is equal to 1 means chaotic perturbation. In certain cases the one or the other specification works better. Different specifications of parameters may suit different types of functions or dimensions – one has to do some trial and error.

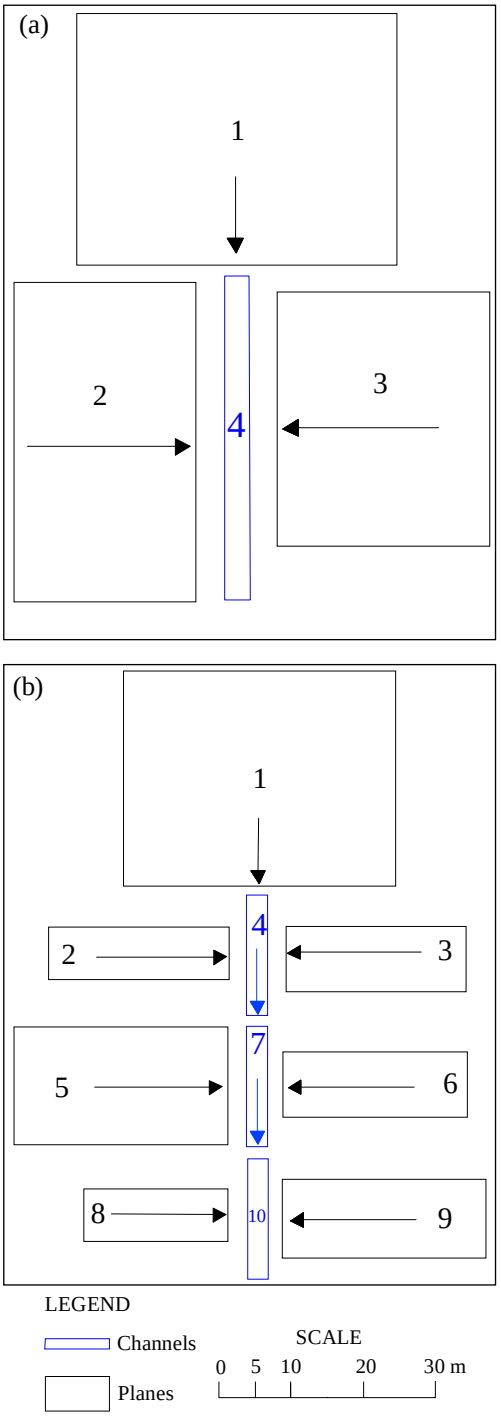

Fig. 2 Different divisions of the MCN3 in plane and channel elements: (a) 4 elements and (b) 10 elements.

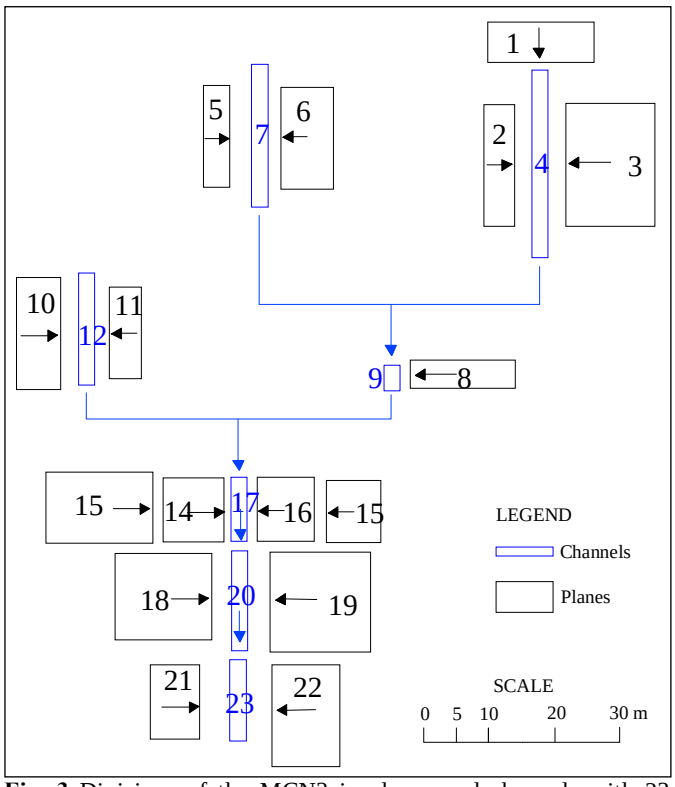

Fig. 3 Divisions of the MCN3 in planes and channels with 23 elements.

Application of the WESP model

The Sumé Experimental Basin became operative in 1982 and since then more than 200 events of precipitation resulting in surface runoff have been documented. This number is large enough for a sediment yield analysis, however the events producing very small runoff are far too numerous than events that resulted in significant runoff and erosion losses, in addition, the range of observation is not uniform.

The trend and the comparative aspects for catchment, however, seem to be quite well established and hence the situation seems to be appropriate for testing and verification of suitable models (Santos *et al.*, 2011).

For the MCN3, 44 precipitation events that occurred between 1987 and 1991 were individually calibrated for erosion. For all the events, the starting values of the three parameters (a, K_r and K_I) were the same, and the maximum, minimum and mean values obtained are shown in **Table 2**. Only three events (204, 206 and 217) had their values of hydraulic conductivity (K_s) changed to respectively 2, 1 and 1mm/h, in order to obtain a calculated runoff event.

The range in which these parameters may vary was chosen as follows: a (0.0001–0.1 kg/m²), K_r (0.1–10.0 kg·m/N$^{1.5}$·s), and K_I (0.1 × 10^8–10.0 × 10^8 kg/s/m^4). **Table 2** shows the statistical analysis for the three parameters as a result of WESP model calibration with the RPS method optimization. It has been observed that the rainfall impact erosion parameter K_I is relatively insensitive with very high values and can be conveniently fixed at a single value, as also observed by Srinivasan *et al.* (2003). Its standard deviation were more significant, ranging from 2.59 (n_2) to 2.62 (n_3).

In the case of the other erosion parameter K_r, the variation also can be considered fairly small, with an average value of 1.69 (n_1), 1.78 (n_2) and 2.10 kg·m/N$^{1.5}$·s^1 (n_3) (**Table 2**). This parameter applies only to erosion on planes, and is a fairly sensitive one. It has been observed that this soil erodibility parameter is affected by antecedent soil moisture conditions and other physical factors such as the slope (Srinivasan *et al.*, 2003). Hence, it is unlikely that this parameter can be regionally represented by a single value. However, if this parameter can be adequately correlated to such local physical factors as slope, length of ramp, and perhaps, a soil moisture index, it should be possible to obtain applicable values for this parameter, within a homogenous hydrological region.

About the channel erosion parameter a, it showed only a very small variation in its range, and would be dependent essentially on the type of soil in the catchment. Its average value was 0.0985 kg/m²; some additional data, from other catchments, would be necessary to confirm whether this can serve as a regional value.

It can be seen that with the discretization n_2, the results showed fewer events with calculated values overestimated or underestimated. A better event calibration is also possible when the discretization is refined, which is the case of n_3. However, a very detailed discretization may unnecessarily increase the modeling uncertainty.

Figure 4 shows the relationship between observed and calculated sediment yield using RPS algorithm for the three ways of discretization of MCN3: (a) 4 elements, (b) 10 elements, and (c) 23 elements. In **Fig. 4a**, it is observed that there were overestimation for sediment yield in nine events.

Table 2. Maximum, average, minimum, standard deviation and mean deviation parameters a, K_r and K_I. using RPS method of optimization

	Max.	Average	Min.	SD[1]	MD[2]
		Discretization n_1			
a	0.0954	0.0098	0.0003	0.0215	0,0128
K_r	2.93	1.69	1.00	0.65	0,59
K_I	9.87	4.53	0.18	2.87	2,50
		Discretization n_2			
a	0.1000	0.0143	0.0003	0.0251	0,0150
K_r	2.96	1.78	1.01	0.59	0,51
K_I	9.96	4.74	0.18	2.59	2,11
		Discretization n_3			
a	0.1000	0.0347	0.0003	0.0352	0,0285
K_r	2.97	2.10	1.01	0.58	0,48
K_I	9.27	3.69	0.40	2.62	2,07

[1] Standard deviation. [2] Mean deviation.

There was also an underestimation of the simulated values for one event, not visible in the graph due to its small value compared to most events.

In general, the pattern of errors indicates global overestimation and underestimation compared to the regression line. **Figure 4b** shows that there were less overestimation for the simulation of sediment yield, when only two events were overestimated. **Figure 4c** shows that, there were less overestimation for the calculated sediment yield events, in which only two values were overestimated.

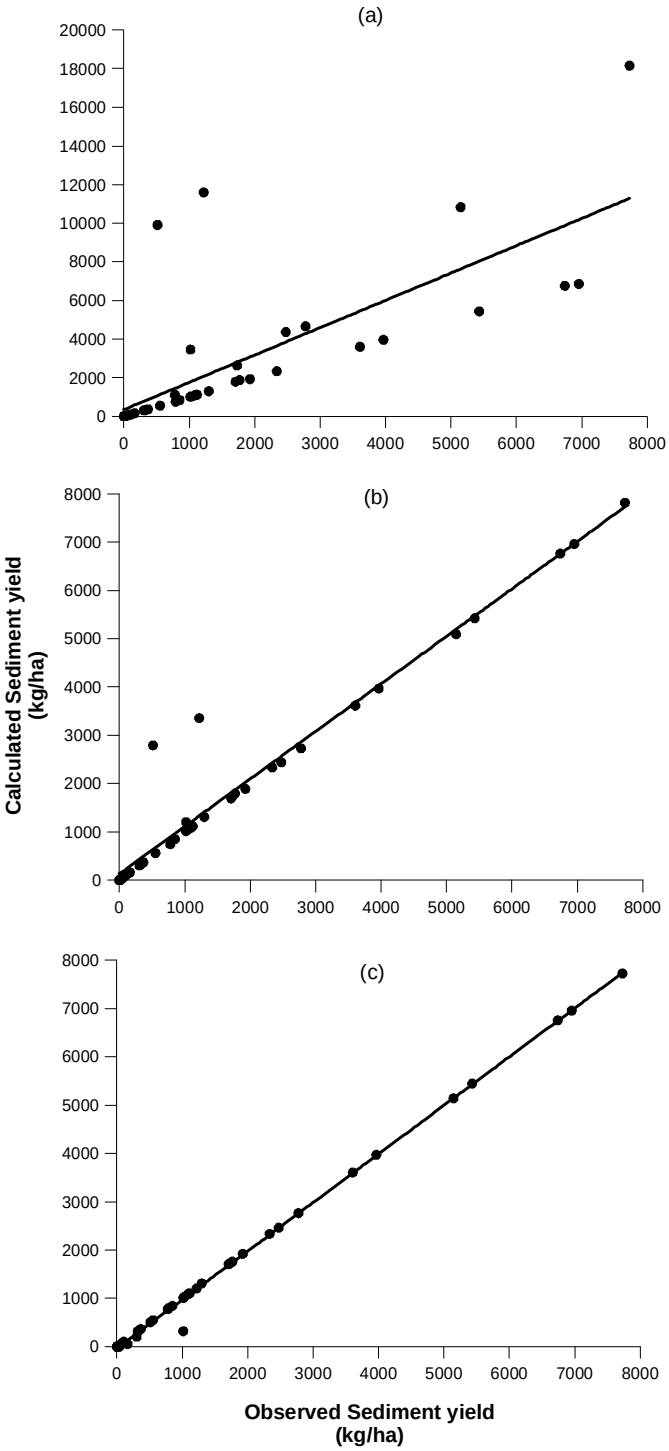

Fig. 4 Relationship between observed and calculated sediment yield using RPS algorithm: (a) discretization n_1, (b) discretization n_2 and (c) discretization n_3.

Event 160 was again the only one to have its value underestimated. Most simulated values were close to or exactly on the equality line, the result of a more accurate calibration. Scatter plots of the errors as ratios of observed and calculates sediment yield produced by RPS method is shown in **Fig. 5**.

The reason for the apparent discrepancy in the mean relative error values is that the highest sediment yield peaks are influenced by the resolution subdivisions of the catchment. The mean relative error for each simulated event using the average values of the erosion parameters into WESP model for the discretizations n_2 and n_3 are relatively low, generally resulting in similar values for these subdivisions, which was not the case of discretization n_3.

Table 3 shows the parameters a, K_r and K_I, optimized for 34 rainfall events with sediment yields E_0 larger than 100 kg/ha, which are assumed to be more accurate than those less than 100 kg. Three parameters a, K_r and K_I should be constant for all rainfall events because they are characterized by sand and soil in the test basin. The orders of these optimized parameters for all the rainfall events seem to be equal for the 23 elements division, but for the 4 and 10 elements division variations of these values are relatively large. The average values of the parameters over the events can become the values for the specific test field. That is for the 23 elements discretization: a = 0.002 (kg·m²/N$^{1.5}$·s), K_r = 2.03 (kg·m/N$^{1.5}$·s), $K_I = 3{\cdot}98 \times 10^8$ (kg·s/m^4).

Figure 6 shows the comparison between observed and calculated sediment yield, for the 35 selected events with observed sediment yield larger than 100 kg/ha. Simulation is done with the average values of a, K_r and K_I for each way of discretization. The calculated values for sediment yield seem to be the same as the observed ones in several events, except for events 152, 177, 179, 187, 198, 229, 239, 246 and 254. There are small differences of calculated values when comparing the three ways of basin division, although the 23 elements division seems to give the best results.

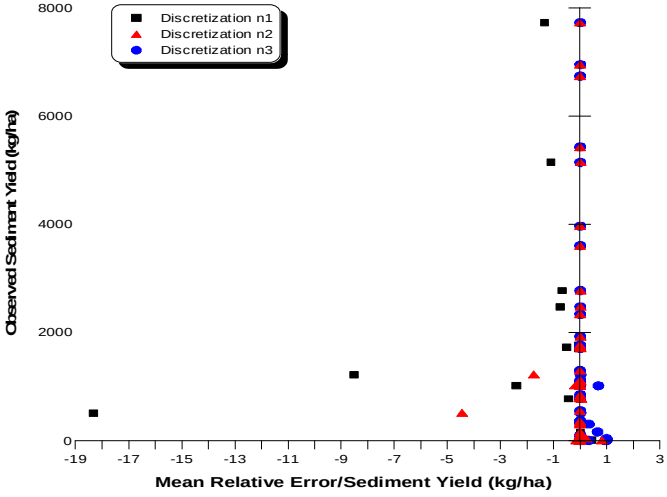

Fig. 5 Scatter plots of errors as ratios of observed sediment yield and mean relative error for the three discretizations in MCN3.

Table 3. Optimized values of parameters with data of E_o > 100 kg

Event	E_o	a (kg·m²/N$^{1.5}$·s)			K_r (kg·m/N$^{1.5}$·s)			$K_I \times 10^8$ (kg·s/m^4)		
		Discretization								
		n_1	n_2	n_3	n_1	n_2	n_3	n_1	n_2	n_3
152	1218.88	0.0003	0.0004	0.0014	1.14	1.10	1.56	3.46	3.59	3.27
155	2335.62	0.0334	0.0264	0.0592	1.67	2.50	2.24	8.44	0.48	4.10
159	323.43	0.0041	0.0056	0.0127	2.25	1.65	2.35	2.46	8.39	4.50
161	5430.19	0.0161	0.0129	0.0294	1.25	2.59	1.01	9.87	2.20	4.03
162	3965.12	0.0104	0.0127	0.0260	1.57	1.56	2.54	6.62	6.60	3.14
165	1093.25	0.0238	0.0208	0.0505	2.90	1.02	2.38	6.91	1.85	9.00
167	1924.58	0.0062	0.0065	0.0163	2.26	2.18	2.84	2.39	5.82	4.37
168	1099.05	0.0029	0.0054	0.0130	2.09	1.39	2.36	3.74	4.95	5.34
172	3606.79	0.0025	0.0115	0.0256	2.54	1.69	1.07	5.92	1.50	7.53
174	1115.53	0.0176	0.0149	0.0316	1.35	2.63	2.94	7.33	7.57	4.40
177	7728.92	0.0005	0.0017	0.0129	1.10	1.25	2.06	0.18	7.23	3.52
178	6952.69	0.0003	0.0065	0.0203	1.14	2.07	2.85	3.46	6.37	3.95
179	2474.33	0.0007	0.0003	0.0089	1.00	1.92	2.45	0.75	5.92	9.27
183	6739.52	0.0017	0.0129	0.0273	2.76	1.60	1.48	3.22	0.81	6.30
184	849.51	0.0105	0.0109	0.0227	2.14	1.42	1.93	8.89	9.96	2.33
186	1706.52	0.0037	0.0033	0.0114	1.12	2.96	1.96	9.33	7.96	1.61
187	1727.83	0.0003	0.0019	0.0068	1.14	1.68	2.79	3.46	4.18	4.14
191	160.70	0.0328	0.0436	0.1000	1.16	1.38	2.34	7.65	6.08	0.40
197	1766.35	0.0005	0.0028	0.0087	1.10	1.76	1.38	0.18	3.41	5.66
198	5146.97	0.0007	0.0011	0.0061	1.00	1.28	2.97	0.75	3.05	5.72
200	1014.43	0.0954	0.0990	0.1000	1.42	1.69	2.34	7.63	6.13	0.40
204	1036.24	0.0009	0.0042	0.0103	2.25	1.21	1.54	5.56	7.27	0.67
206	366.70	0.0003	0.0025	0.0069	1.14	1.33	2.77	3.46	6.35	4.06
210	1296.56	0.0017	0.0065	0.0170	2.03	2.92	1.33	2.89	5.38	6.72
216	322.45	0.0195	0.0163	0.0427	2.68	2.84	1.68	4.94	4.37	5.53
217	551.38	0.0057	0.0061	0.0185	2.45	2.27	1.87	2.35	9.20	2.63
228	789.09	0.0008	0.0017	0.0076	1.06	2.65	1.98	8.10	4.28	1.94
229	1016.71	0.0005	0.0003	0.0022	1.10	1.14	1.22	0.18	3.46	6.85
239	777.61	0.0004	0.0017	0.0058	1.10	1.25	2.32	2.20	7.23	2.44
246	512.77	0.0005	0.0005	0.0003	1.10	1.10	1.14	0.18	0.18	3.46
253	2776.25	0.0003	0.0021	0.0088	1.14	1.49	1.07	3.46	5.05	2.02
254	304.58	0.0325	0.0371	0.1000	2.93	1.01	2.34	2.19	4.33	0.40
263	104.62	0.0080	0.0088	0.0309	2.80	1.07	2.83	6.36	4.32	2.99
264	472.19	0.0003	0.0016	0.0053	1.14	2.03	1.22	3.46	9.65	2.65
Average	1083.27	0.0100	0.0100	0.0200	1.68	1.75	2.03	4.35	5.15	3.98

The calculated values for sediment yield seem to be the same as the observed ones in several events, except for events 152, 177, 179, 187, 198, 229, 246, and 253. There are small differences of calculated values when comparing the three ways of basin division, although the 23 elements division seems to give the best results.

In order to differentiate further in deciding on the suitability of the three remaining discretizations (4, 10 and 23 elements), the **Table 4** shows the variation of the observed and calculated sediment yield in 34 optimization runs of the WESP model using optimization method. It may be observed that for the Discretization with 23 elements, the variations of the statistical values in successive tests are small in comparison to the other discretizations and the values of are generally the lowest. This indicates that the discretization with little number of elements not produce similar efficiency values for calculated sediment yield like the discretization with considerable number of elements.

Table 4. Comparative assessment between observed and calculated sediment yield in 34 optimization runs of the WESP model using optimization method

Discretization	EMR	R^2	RMSE	MSE
n_1	-76.45	0.69	51.80	57.27
n_2	18.84	0.90	19.21	7.88
n_3	4.88	0.99	7.64	1.25

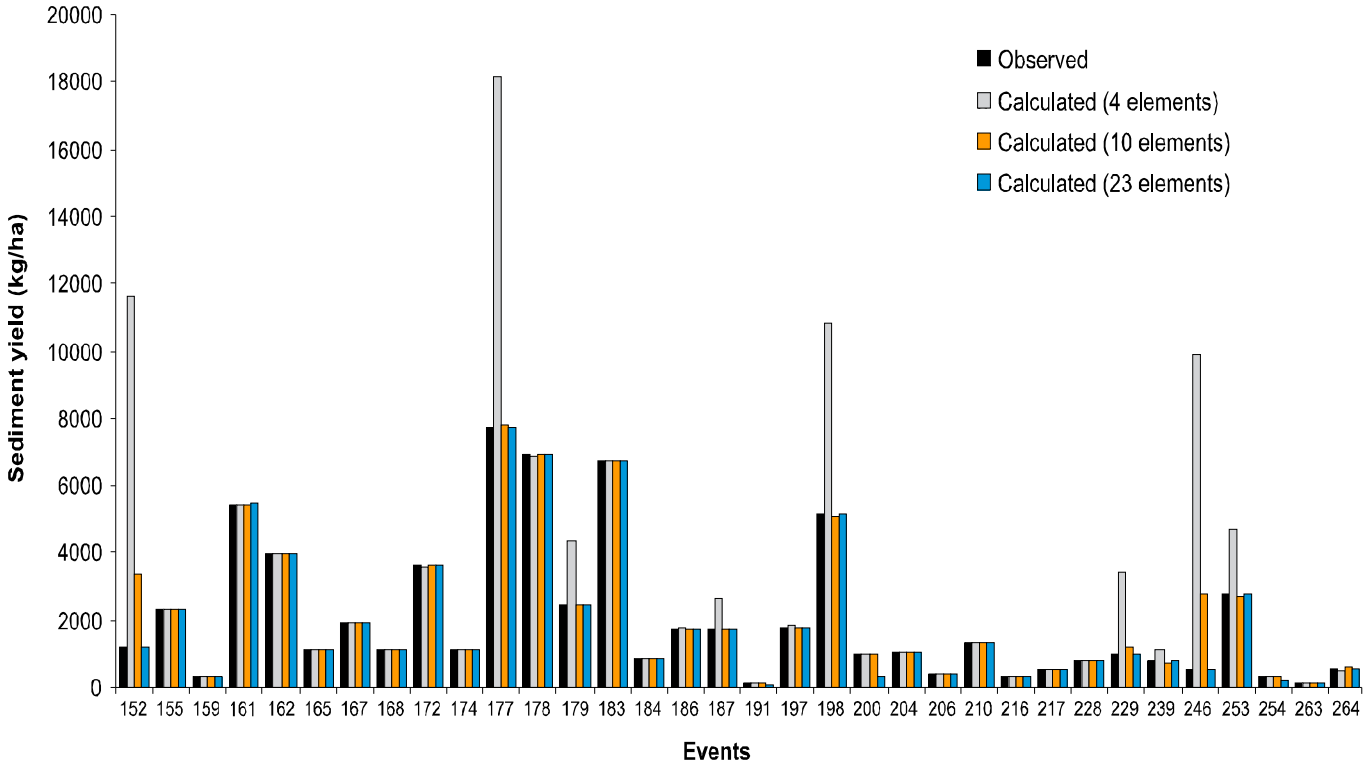

Fig. 6 Observed and calculated sediment yield with data E_o > 100 kg/ha.

CONCLUSION

In order to compare the influence of the basin discretion on the runoff-erosion simulation, the Repulsive Particle Swarm (RPS), which is a population based stochastic optimization technique, inspired by social behavior of bird flocking or fish schooling, was applied to a physically-based runoff-erosion model named WESP. The results show that though optimized parameter values are different according to the discretization, they are within the range of acceptance. Although, the 23 elements discretization shows the best results, 10 elements discretization seems also to give an acceptable simulation performance.

REFERENCES

Bingner, R.L., Garbrecht, J., Arnold, J.G. & Srinivasan, R. (1997) Effect of watershed subdivision on simulation runoff and fine sediment yield. *Trans. ASAE* **40**(5), 1329–1335.

Cadier, E., Freitas, B.J. & Leprun, J.C. (1983) *Bacia Experimental de Sumé: instalações e primeiros resultados*. SUDENE, Recife, PE, Brazil.

Croley II, T.E. (1982) Unsteady overland sedimentation. *J. Hydrol.* **56**(4), 325–346. doi: 10.1016/0022-1694(82)90021-X

Davis, S.S. (1978) Deposition of nonuniform sediment by overland flow on concave slopes. *MSc. Thesis*, Purdue University, West Lafayette, IN, 137 p.

Duan, Q., Sorooshian, S. & Gupta, V. (1992) Effective and efficient global optimization for conceptual rainfall-runoff models. *Water Resour. Res.* **28**(4), 1015–1031. doi: 10.1029/91WR02985

Eberhart, R.C. & Kennedy, J. (1995) A new optimizer using particle swarm theory. *Proc. 60th Symposium on Micro Machine and Human Science* (IEEE Service Center, Piscataway, NJ, USA), 39–43.

Einstein, H.A. (1968) Deposition of suspended particles in a gravel bed. *J. Hydraulic Div. ASCE* **94**(5), 1197–1205.

Elshorbagy, A., Simonovic, S.P. & Panu, U.S. (2000) Performance evaluation of artificial neural networks for runoff prediction. *J. Hydrol. Engng.* **5**(4), 424–427. doi: http://dx.doi.org/10.1061/(ASCE)1084-0699(2000)5:4(424)

Foster, G.R. (1982) *Modeling the erosion process*. In: Haan, C.T., Johnson, H.P. & Brakensiek, D.L. (Eds.). Hydrologic modeling of small watersheds, Am. Soc. Agr. Eng., 295–380.

Gandolfi, C. & Bischetti, G.B. (1997) Influence of the drainage network identification method on geomorphological properties and hydrological response. *Hydrol. Process.* **11**(4), 353–375. doi: 10.1002/(SICI)1099-1085

Green, W.H. & Ampt, G.A. (1911) Studies on soil physics, I. The flow of air and water through soils. *J. Agr. Sci.* **4**(1), 1–24.

Helmlinger, K.R., Kumar, P. & Foufoula-Georgiou, E. (1993) On the use of digital elevation model data for Hortonian and fractal analyses of channel networks. *Water Resou. Res.* **29**(8), 2599–2613. doi: 10.1029/93WR00545

Kalin, L., Govindaraju, R.S. & Hantush, M.M. (2003) Effect of geomorphologic resolution on modeling of runoff hydrograph and sedimentograph over small watersheds. *J. Hydrol.* **276**(1), 89–111. doi: 10.1016/S0022-1694(03)00072-6

Laloy, E., Fasbender, D. & Bielders, C.L. (2010) Parameter optimization and uncertainty analysis for plot-scale continuous modeling of runoff using a formal Bayesian approach. *J. Hydrol.* **380**(1), 82–93. doi: 10.1016/j.jhydrol.2009.10.025

Lane, L.J. & Shirley, E.D. (1985) *Erosion and sediment yield equations: solutions for overland flow*. Workshop on USLE Replacement, Nat. Soil Erosion Lab., West Lafayette, IN, p. 22.

Lopes, V.L. & Lane, L.J. (1988) Modeling sedimentation processes in small watersheds. *IAHS Publ.* **174**, 497–508.

Mazion Jr., E. & Yen, B.C. (1994) Computational discretization effect on rainfall-runoff simulation. *J. Water Resour. Plann. Manage.* **120**(5), 715–734. doi: 10.1061/(ASCE)0733-9496(1994)120:5

Mehta, A.J. (1983) Characterization tests for cohesive sediments. *Proc. Conference on Frontiers in Hydraulic Engineering.* ASCE/MIT, Cambridge, Mass., 79-84.

Morris, G.D. & Heerdegen, R.G. (1988) Automatically derived catchment boundaries and channel networks and their

hydrological applications. *Geomorph.* **1**(2), 131–141. doi: 10.1016/0169-555X(88)90011-6

Nash, J.E. & Sutcliffe, J.V. (1970) River flow forecasting through conceptual models, Part I –A discussion of principles. *J. Hydrol.* **10**(3), 282–290. doi: http://dx.doi.org/10.1016/0022-1694(70)90255-6

Rigon, R., Rinaldo, A., Rodriguez-Iturbe, I., Bras, R.L. & Ijjasz-Vasquez, E. (1993) Optimal channel networks: a frame-work for the study of river basin morphology. *Water Resou. Res.* **29**(6), 1635–1646. doi: 10.1029/92WR02985

Rinaldo, A., Rodriguez-Iturbe, I., Rigon, R., Bras, R.L., Ijjasz-Vasquez, E. & Marani, A. (1992) Minimum energy and fractal structures of drainage networks. *Water Resou. Res.* **28**(9), 2183–2195. doi: 10.1029/92WR00801

Rodriguez-Iturbe, I., Ijjasz-Vasquez, E., Bras, R.L. & Tarboton, D.G. (1992) Power law distribution of mass and energy in river basins. *Water Resou. Res.* **28**(4), 1089–1093. doi: 10.1029/91WR03033

Santos, C.A.G., Freire, P.K.M.M., Arruda, P.M. & Mishra, S.K. (2011a) Application of a differential evolution optimizer to the tank model. In: XIVth IWRA World Water Congress, 2011, Porto de Galinhas. *Proc. 14th IWRA World Water Congress*. Montpellier: International Water Resources Association, 1–6.

Santos, C.A.G., Freire, P.K.M.M., Mishra, S.K., Soares Júnior, A. (2011b) Application of a particle swarm optimization to the tank model. *IAHS Publ.* **347**, 114–120.

Santos, C.A.G., Pinto, L.E.M., Freire, P.K.M.M. & Mishra, S.K. (2010) Application of a particle swarm optimization to a physically-based erosion model. *Land Reclam.* **42**(1), 39–49. doi: 10.2478/v10060-008-0063-9

Santos, C.A.G., Srinivasan, V.S. & Silva, R.M. (2005) Evaluation of optimized parameter values of a distributed runoff–erosion model applied in two different basins. *IAHS Publ.* **292**, 101–109.

Santos, C.A.G., Srinivasan, V.S., Suzuki, K. & Watanabe, M. (2003) Application of an optimization technique to a physically based erosion model. *Hydrol. Process.* 17(5), 989–1003. doi: 10.1002/hyp.1176

Simon, H.A. (1982) *Models of bounded rationality*. Cambridge University. Press, Cambridge, MA, USA.

Snell, J.D. & Sivapalan, M. (1994) On the geomorphologic dispersion in natural catchments and geomorphological unit hydrograph. *Water Resou. Res.* **30**(7), 2311–2323. doi: 10.1029/94WR00537

Soares Júnior, A., Santos, C.A.G., Motta, G.H.M.B., Barbosa, F.A.R., Freire, P.K.M.M. (2010a) Application of an XML-based genetic algorithm in to a rainfall-runoff erosion model. *IAHS Publ.* **337**, 366–374.

Soares Júnior, A.L., Farias, C.A.S., Santos, C.A.G. & Suzuki, K. (2010b) An XML-based genetic algorithm tool: application for the calibration of a Tank model. *Proc. 17th Congress of the Asia and Pacific Division of the International Association of Hydraulic Engineering and Research*. Auckland: IAHR, 1–10.

Srinivasan, V.S. & Galvão, C.O. (1995) Evaluation of runoff and erosion loss in microbasins utilizing the hydrodynamic model WESP. *Adv. Engn. Softw.* **22**(2), 79–85. doi: 10.1016/0965-9978(95)00014-N

Srinivasan, V.S. & Paiva, F.M.L. (2009) Regional validity of the parameters of a distributed runoff-erosion model in the semi-arid region of Brazil. *Sci. China Series E: Technol. Sci.* **52**(11), 3348–3356. doi: 10.1007/s11431-009-0345-4

Srinivasan, V.S., Aragão, R., Suzuki, K. & Watanabe, M. (2003) Evaluation of an erosion simulation model in a semiarid region of Brazil. *IAHS Publ.* **279**, 109–116.

Srinivasan, V.S., Gomes, H.P., Leprun, J.C. & Silva, I.G. (1988) Erosion studies in Sumé – a semi-arid region in the northeast of Brazil. *IAHS Publ.* **174**, 307–314.

Tarboton, D.G., Bras, R.L. & Rodriguez-Iturbe, I. (1991) On the extraction of channel networks from digital elevation data. *Hydrol. Process.* **5**(1), 81–100. doi: 10.1002/hyp.3360050107

Thieken, A.H., Lücke, A., Diekkruger, B. & Richter, O. (1999) Scaling input data by GIS for hydrological modelling. *Hydrol. Process.* **13**(4), 611–630. doi: 10.1002/(SICI)1099-1085

Urfalioglu, O. (2004) Robust estimation of camera rotation, translation and focal length at high outlier rates. *Proc. I Canadian Conference on Computer and Robot Vision.* Washington, DC, USA), 464–471.

Vieux, B. & Needham, S. (1993) Nonpoint-pollution model sensitivity to grid cell size. *J. Water Resour. Plann. Manage.* **119**(2), 141–157. doi: 10.1061/(ASCE)0733-9496

Zhang, W. & Montgomery, D.R. (1994) Digital elevation model grid size, landscape representation, and hydrologic simulations. *Water Resou. Res.* **30**(4), 1019–1028. doi: 10.1029/93WR03553